ORIGINAL ARTICLE

INVESTIGATING THE MECHANISMS OF U(VI) SORPTION ONTO FE(0) AND SHEWANELLA PUTREFACIENS SURFACES IN THE PRESENCE OF AS(V) USING EXTENDED X-RAY ABSORPTION FINE STRUCTURE SPECTROSCOPY

| Clement N'zau Umba-di-Mbudi [1*] |

[1.] Université de Kinshasa | Département de geosciences | Groupe Geo-Hydro-Energie | Kinshasa, RD Congo |

| Received May 19, 2020 | | Accepted May 26, 2021 | | Published June 01, 2021 | | ID Article | Clement-Ref6-ajira210521|

ABSTRACT

Background: Sorption processes control the mobility, biodisponibility, bio-transformation, speciation and ultimately the toxicity of metals and metalloids in the subsurface. **Methods**: This paper analyses the electronic and geometric structure of solid samples of uranium onto scrap metallic iron and the versatile bacterium Shewanella putrefaciens surfaces in the presence of arsenic by means of U L3 and As K- edge extended X-ray absorption fine structure (EXAFS) measurements prepared by batch sorption experiments. **Results**: This analysis complements a companion XANES fingerprinting investigation both aiming at uncovering the underlying major mechanism controlling the state of the uranium atoms. The sorption experiment samples comprise of the systems Fe(0)-0.1 mM U, Fe(0)-0.1 mM U-0.1 mM As and the anoxic Fe(0)-0.1 mM U-0.1 mM As-DSMZ Shewanella putrefaciens strain 6067 at concentration of two optical density units (600 nm) equilibrated for 24 hours in the dark without shaking. EXAFS spectra evaluation confirms the presence and prevalence of respectively U(VI)-O/O-OH axial and equatorial bonds in the mono-component uranium system and both U(VI)-O/O-OH and tetrahedron As(V)-(O,OH) in the bi-components uranium–arsenic systems sorbed onto scrap metallic iron and Shewanella putrefaciens surfaces. **Conclusion**: The absence of peaks beyond the major axial and equatorial U(VI)-O/O-OH bonds in the mono-component uranium system and the concurrent occurrence of U(VI)-O/O-OH and As(V)-(O,OH) bonds in the bi-component uranium-arsenic systems suggest the likely plausibility of precipitation/co-preciptation mechanism as the leading control of uranium behavior.

Keywords: *sorption, uranium, arsenic, XAFS, modeling, iron, bacteria.*

1. INTRODUCTION

Sorption processes control the mobility, biodisponibility, bio-transformation, speciation and ultimately the toxicity of metals and metalloids in the subsurface [1, 2, 3]. They play a capital role in contaminant hydrogeology, reactive transport and site remediation. Thus, a sound understanding and prediction of the specific sorption mechanisms regulating the fate of contaminants of concerns such as uranium and arsenic in the subsurface is paramount in the design of a remediation technology such as a permeable reactive barrier.

Uranium and arsenic sorption onto metallic iron and corrosion products as well as onto bacteria surfaces have gained much interest among environmental technologists, scientists and engineers owing partly to the former strong redox potentials and the latter high surface area. Besides, over the last decades, some bacteria have been recognized as uranium and arsenic scavengers. For instance, dissimilatory Fe(III) reducing bacteria such as Geobacter metallireducens and Shewanella putrefaciens have gained attention owing to their capability to couple the oxidation of organic matter to the reduction of Fe(III) and alternatively various metals/metalloids including uranium and arsenic [4, 5]. However, conditions that can inhibit these often presented as enzymatically driven biotransformation processes are still not well known.

As aforementionned, for a contaminated site remediation engineer perspective, a good understanding of the binding mechanisms of uranium and arsenic onto metallic iron and corrosion products as well as onto bacteria surfaces is a key design input for an effective dimensioning and operation of an efficient reactive barrier. To date, however, the mechanistic description of uranium sorption onto metallic iron has been based on hypotheses that include either reductive precipitation induced by elemental Fe(O), structural Fe(II) or even H_2, chemisorption at the surfaces of Fe(O) and corrosion products, precipitation/co-precipitation, or their combination [6,7,8,9,10,11]. Similarly, arsenic sorption onto elemental iron and corrosion products has also been reported either as co-precipitation of the reduced As (III) from As (V) or as adsorption of both As (V) and As (III) on iron corrosion products or other pre-existent oxyhydroxides [12, 13, 14].

Among the large array of interfacial investigation techniques, extended x-ray absorption fine structure (EXAFS) spectroscopy is well suited to elucidate the coordination chemistry and ultimately to better comprehend the binding mechanism of uranium onto elemental iron and corrosion products, and bacteria surfaces in the presence of arsenic. Noteworthy however, despite the well-established EXAFS efficiency in uncovering the binding mechanisms of metals/metalloids on environmental solids [15] (Brown 1990), yet studies trying to decipher uranium fixation onto solids in the presence of arsenic are scarce. Denecke et al., (2005) used EXAFS techniques to assess the mechanisms

that led to the immobilization of uranium in tertiary sediment from a waste disposal natural analogue site in the presence of arsenic either as As(V) or As(0) [16].

Mbudi et al., (2007) discussed the speciation of uranium and arsenic sorbed onto scrap metallic iron and Shewanella putrefaciens surfaces based on x-ray absorption near edge structure (XANES) fingerprinting investigation [19]. This investigation focuses on uncovering the coordination chemistry of uranium and arsenic sorbed onto scrap metallic iron and corrosion products and Shewanella putrefaciens surfaces prepared in no growth and ultimately on conditions that potentially inhibit these bacteria enzymatic capabilities to biotransform uranium and arsenic. To this end, this analysis applies ab initio calculations and least square fitting routines to model bulk EXAFS spectra from batch experiments systems that equilibrated uranium alone with scrap metallic iron, uranium with arsenic in contact with scrap metallic iron and bi-component water containing uranium and arsenic onto scrap metallic iron and Shewanella putrefaciens cells. The coordination chemistries and hence fixation mechanisms of both uranium and arsenic are assessed and compared in these three systems with the ultimate goal of uncovering the influence of arsenic and bacteria on the fate of uranium under experimental conditions.

2. MATERIELS AND METHODES

2.1 Materials

Uranyl nitrate 6-hydrate $UO_2(NO_3)_2.6H_20$ (Chemapol, Germany) and sodium arsenate $Na_2HAsO_4.7H_20$ (Baker, Germany) of analytical grade were used to prepare stock solutions of uranium and arsenic. The reagents used for bacterium growth include yeast extract (Roth, Germany), peptone (VEB Berlin Chemie, Germany) and NaCl (Riedel-de-Haen, Germany). The background electrolyte used in every experiment was prepared from sodium nitrate from Merk (Germany) dissolved in deionized water with a Milli-Q Water Purification System (Millipore, France).

The scrap metallic iron type S69 from Metallaufbereitung Zwickau (Germany) was crushed and sieved. The homogeneous 0.1 mm fraction was used as sorbent. The elemental composition of the selected scrap metallic iron used throughout is 92.8% Fe, 3.5% C, 2.1% Si, 0.9% Mn and 0.7% Cr.

2.2 Bacteria Culturing and Harvesting

The Shewanella putrefaciens bacterium referred to as strain 6067 was purchased as dried culture from Deutsche Sammlung von Mikroorganismen und Zellkulturen GmbH (DSMZ). The strain was resuscitated following routine DSMZ protocol and the active stock was thereafter used to inoculate a Petri dish containing yeast extract, peptone and agar, and incubated at room temperature (about 23°C). Cells culturing was carried out aerobically at similar ambient temperature using a set of 250 ml glass Erlenmeyer filled with 100 ml of the growth medium and inoculated with a loopful of Shewanella putrefaciens colonies from Petri dish. The growth medium comprised 2 g/l yeast extract, 5 g/l peptone and 5 g/l NaCl adjusted to pH 7 with NaOH prior to sterilization. The culture vessels were put on a shaker and incubated at room temperature until the late exponential growth phase. Cells harvesting was achieved through centrifugation at 7000 g for 15 minutes at a temperature of 10°C. The harvested cells were washed twice using a sterile and anoxic 0.01 M KOH solution. The re-suspension of the washed pellets was carried out in anoxic 0.01 M $NaNO_3$ background electrolyte solution of the biotic batch sorption experiment reaction vessel.

2.3 Batch Sorption Experiments

Two samples representing the reacted solid phase from the experimental design systems Fe(0)-0.1 mM U and Fe(0)-0.1 mM U-0.1 mM As were prepared abiotically using 100 ml polyethylene reaction vessels. Each reaction vessel contained 2 g of 0.1 mm particulate sized scrap metallic iron set to equilibrate in a solid to solution ratio (weight/weight) of 1/50 using a background electrolyte solution of 0.01 M $NaNO_3$ spiked respectively with uranium 0.1 mM U alone or with the bi-component 0.1 mM U-0.1 mM As adjusted in either case at pH 4.5. A third sample was prepared from a biotic batch sorption experiment of the system Fe(0)-0.1 mM U-0.1 mM As-bacteria cells. The solutions used in this system were adjusted at pH 4.5 and purged with high purity nitrogen gas prior to sterilization. A 75 ml glass bottle capped with rubber crimped with an aluminium seal as the reaction vessel. It comprised a mixture of 1 g of 0.1 mm scrap metallic iron particles in 50 ml of a 0.01 M $NaNO_3$ background electrolyte solution spiked with Shewanella putrefaciens cells to achieve a concentration of two optical density units (600 nm) at the end of the six hours hydration time imposed to both the abiotic and biotic systems. An enhancement of the reducing conditions was achieved through the addition of high purity ethanol at concentration of 0.05% as electron donor.

The addition of uranium alone or both uranium and arsenic in either the abiotic or the biotic systems, marked the start of the sorption experiment. Photochemical reactions were minimized using aluminum foil to cover the reaction vessels. These vessels were wrists shaken up and down up to ten times at the beginning and left to equilibrate for 24 hours.

2.4 XAFS measurements

XAFS spectra for both bulk U L3 (17.175 keV) and As K (11.867 keV) from selected solid samples of abiotic (Fe(0)-0.1 mM U and Fe(0)-0.1 mM U-0.1 mM As) and biotic (Fe(0)-0.1 mM U-0.1 mM As-bacteria cells) batch sorption

experiments were recorded at the INE-Beamline for Actinide Research (Rothe et al. 2006) at the ANKA synchrotron radiation facility (Karlsruhe, Germany). The ANKA synchrotron storage ring was operating at 2.5 GeV with current intensity spanning 85 and 180 mA. The three selected experimental samples were contained into Eppendorf vials and sealed in polyethylene bags and positioned with a goniometer (Huber Diffraktionstechnik, Germany) with respect to the focused beam of 1mm diameter. The Lemonier type double crystal X-ray monochromator (DCM) equipped with a set of Ge(422) crystals was used with the second crystal detuned to 60% of the maximum intensity for the bulk U L3-edge XAFS measurements whereas a detuning of the second DCM crystal to 70% of the maximum photon intensity was necessary for better bulk As K edge XAFS spectra. The XAFS spectra were recorded in fluorescence mode at ambient temperature (~ 23°C) using a five-pixel low energy fluorescence germanium solid state detector (Canberra). For each of the three samples, nine XAFS scans were recorded for either uranium or arsenic to increase the signal-to-noise ratio.

Schoepite was used as calibration reference for the U-L3-edge excitation energy whereas As K-edge XANES spectra scans of arsenic metal foil [As(0)] and powder samples of $As(III)_2O_3$, and $As(V)_2O_5$ as reference compounds were recorded in transmission mode using argon filled ionization chambers.

2.5 XAFS Data Reduction, ab initio Calculations and Modeling

The XAFS routines from Athena software package (Ravel and Newville, 2005) was used throughout for the XAFS scans spectra averaging, background subtraction and normalization following standard procedures. To this end, uranium spectra were calibrated and aligned with respect to the first inflection point of the first derivative of the Schoepite spectrum while arsenic spectra were similarly calibrated with respect to As(0). The resulting merged and reduced χ(k) was imported into the Artemis XAFS data modeling software package (Ravel and Newville 2005). Ab inito calculations which include scattering amplitudes and phases as well as the determination of potentials and Fermi level were carried out using the FEFF6 embedded within Artemis. The input file for FEFF6 was prepared with ATOMS crystallographic software also embedded within Artemis using space groups and related crystallographic of Schoepite, Heinreichite and Abernathyite from the American Mineralogist Crystal Structure Database (AMCSD) for respectively the Fe-U, Fe-U-As and Fe-U-As-bacteria cells but Abernathyite for the arsenic spectrum of Fe-U-As-bacteria cells system.

3. RESULTS

The respective uranium and arsenic spectra are described and discussed qualitatively with respect to reference compounds followed by a quantitative analysis of structural parameters derived from ab initio calculations and experimental data fitting. Overall, as already shown for the XANES fingerprinting companion study [19], the EXAFS experimental data for both uranium and arsenic do show structural characteristic details consistent with known U(VI) and As(V) respective coordination chemistry in the oxides as shown in oxides reference compounds.

3.1 Qualitative Spectral Analysis

3.1.1 Uranium: The normalized and background substracted EXAFS spectra derived from the full XAFS spectra are presented in k space χ(k) and in R space with the corresponding Fourier transform (FT) and, backward FT spectra of the sorption experiment compared to Schoepite in figures 1a, 1b and 1c considering for the calculations the k range of 2 A^{-1} to around 12 A^{-1}.

At low k values of all three aforementionned figures (the χ(k), FT and backward FT spectra) the waves pattern of sorption experiment samples is in general similar to the Schoepite reference sample for the full spectra. In detail, however, worth noting the close similarity of the FT spectra of the Fe-U system to the Schoepite spectrum compared to the slightly different FT waves patterns exhibit by the Fe-U-As and Fe-U-As-bacteria cells systems particularly in the 1-3 Å range.

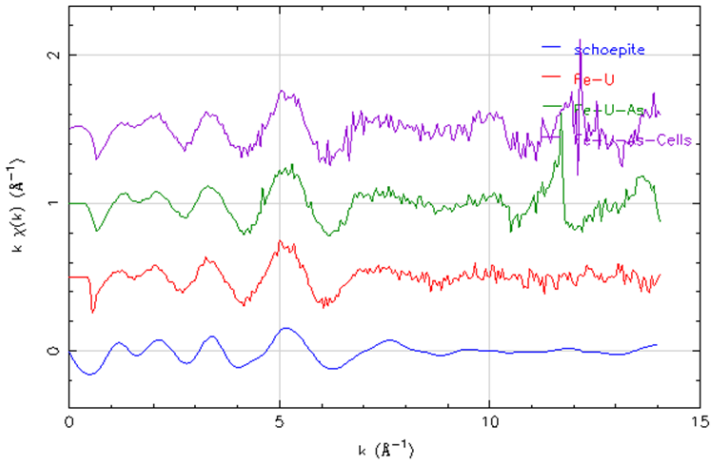

Figure 1a: A comparison of the normalized and background subtracted χ(k) of the sorption experiment samples spectra to the reference Schoepite spectrum.

At higher k values of at leat 10 A^{-1}, both the χ(k) and subsequently the backward FT show a wave pattern with highest peaks of χ(k) at 11.5 A^{-1} and 12 A^{-1} only found in respectively both bi-components uranium-arsenic systems Fe-U-As and Fe-U-As-bacteria cells systems.

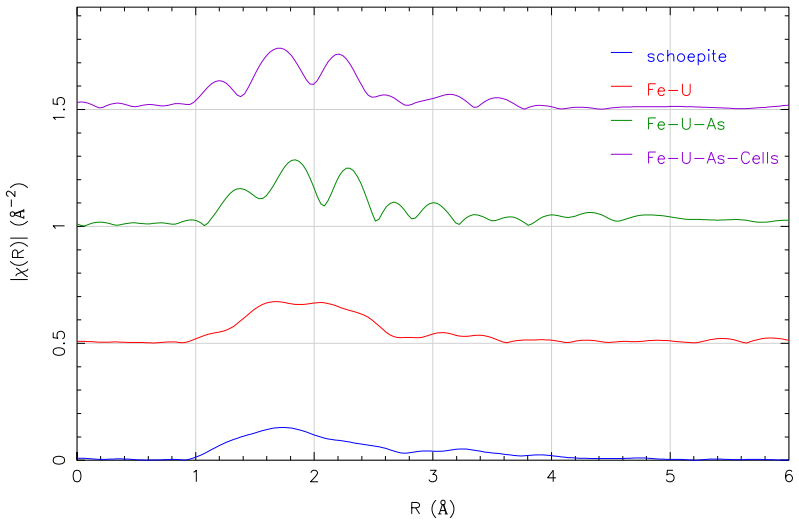

Figure 1b: Comparing Fourier transformed χ(k)-spectra of experimental samples to Schoepite.

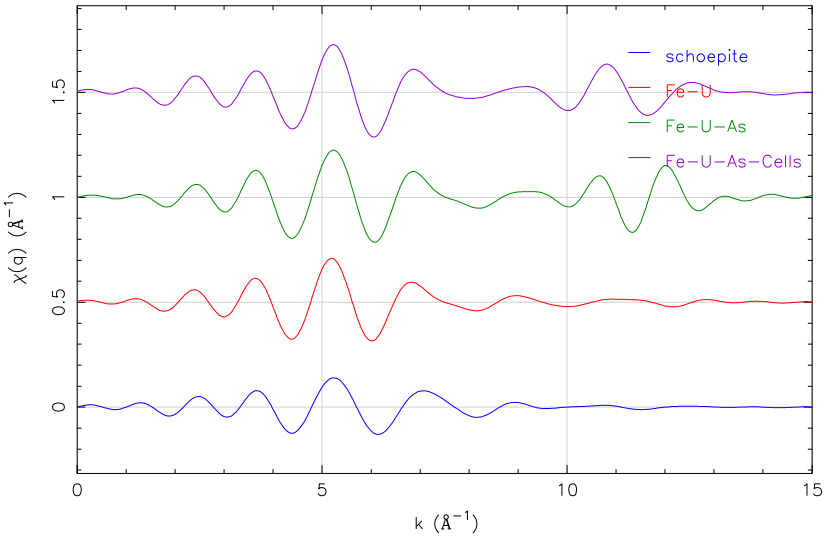

Figure 1c: Backward Fourier transforms of experimental samples compared to Schoepite.

Whether these higher peaks hold some structural information or just experimental artifacts is difficult to precisely pinpoint since modeling very higher shells coordination chemistry is not straightforward either. Thus, a comparison of respective k-weighted 1,2 and 3 for the k range 3-10 Å presented as weighted 3 of the FT is shown in figures 1d, 1e and 1f.

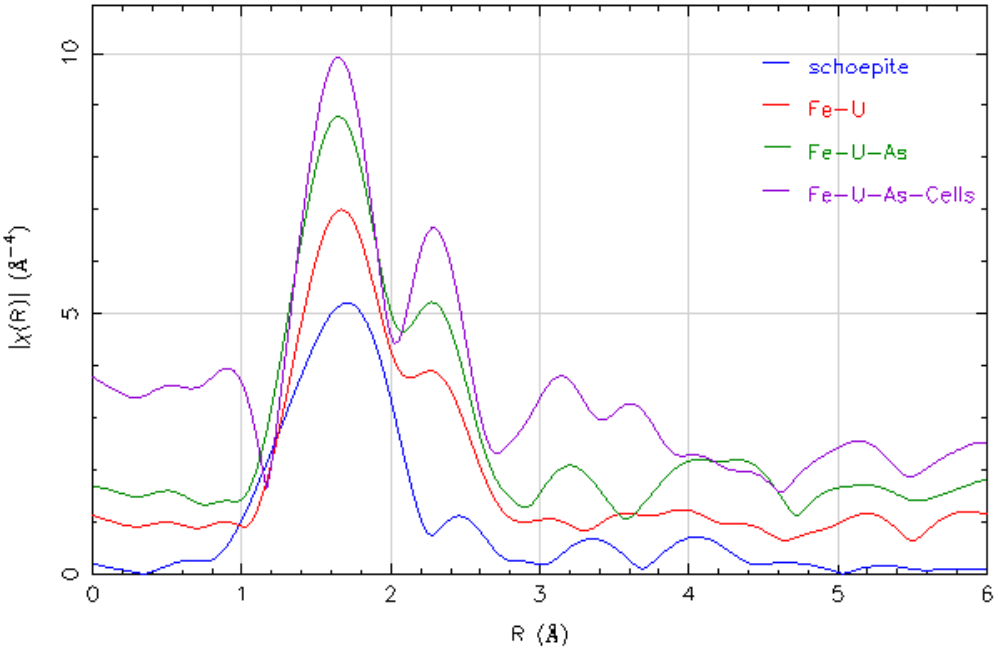

Figure 1d: Fourier transforms of uranium spectra compared to schoepite spectrum for the k range 3-10 Å weighted by k = 3.

The magnified and phase shifts corrected FT shown in figures 1d through 1f consider the k range 3-10 Å to avoid the apparent artifacts or uneasy to decipher structural information aforementionned at higher k values. It clearly appears from these figures a first peak signal at 1.6-1.8 Å which corresponds to the two shorter bound axial oxygen atoms aligned with uranium (VI) as they are comparable to the Schoepite spectrum. This U-O coordination shell is recognizable in all three sorption experiment samples.

While the second peak of the three sorption experimental samples are equally well aligned, they seem however, slightly left shifted at 2.38-2.4 Å compared to the schoepite second peak at around 2.44 Å. The location of the third peak for both arsenic containing experimental samples are similarly aligned around 3.2 Å contrasting with the Schoepite third shell at around 3.4 Å and the Fe-U system third shell barely recognizable between 3-3.2 Å. The overall amplitudes of the peak though as shown in figure 1d, grow higher from Schoepite to the Fe-U, Fe-U-As and Fe-U-As-bacteria cells systems.

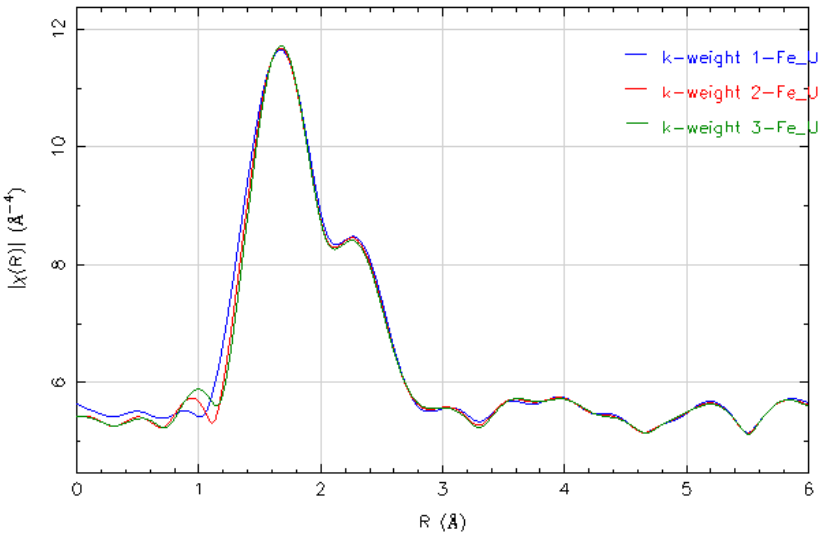

Figure 1e: Comparing k-weights 1-2-3 of Fourier transformed uranium spectra in the Fe-U system for the k range 3-10 Å.

In addition, figures 1e and 1f are illustrative of the attempt to check the sensibilities of the second and third shells amplitudes with changing k-weighted values respectively k=1, 2 and 3 in order to qualitatively determine the possible type of scattering atom since high atomic number atom such as U usually increase amplitude with increasing k-weight while low atomic number reverse the trend. Thus, consistent with the most likely presence of O/OH equatorial bond in

the second shell for all experimental sorption samples, there are apparently none high Z atom such as U in the third shells but possibly a relatively low Z atoms such as As, Fe or O.

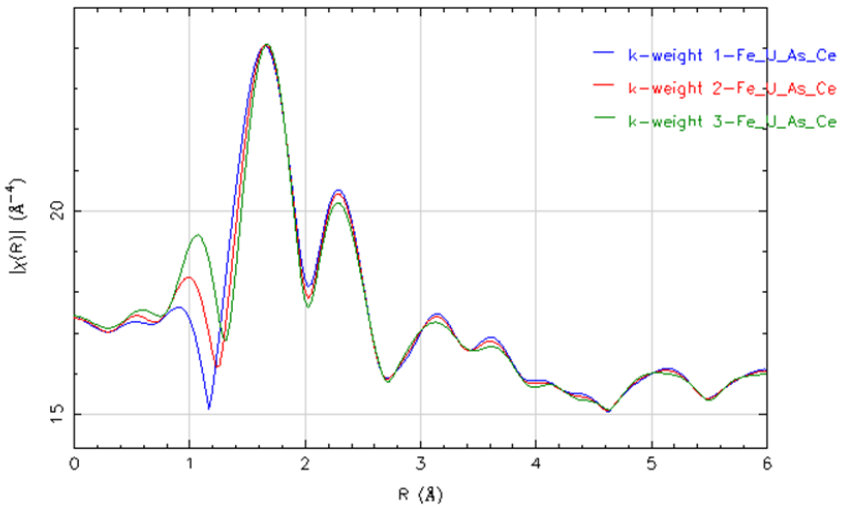

Figure 1f: Comparing k-weights 1-2-3 of Fourier transformed uranium spectra in the Fe-U-As-bacteria systems for the k range 3-10 Å.

Overall, knowing the oxidation state 6 of all uranium spectra as shown in XANES fingerprinting in Mbudi et al., (2007), it can be inferred from similarities with known Schoepite FT EXAFS features as well as from related literature that the first peak correspond most likely to the U-O axial and linear bonds while the second peak is the would be signature of the U-O equatorial bonds [19].

3.1.2 Arsenic

Similar to the uranium qualitative analysis above, the normalized, background subtracted χ(k), FT and backward FT of arsenic spectra are presented in figures 2a through 2f. While figure 2a compares only arsenic containing sorption experimental spectra Fe-U-As and Fe-U-As-bacteria cells systems for the full XAFS range, figures 2b to 2d include arsenic standards XANES portion converted in k space and R space and hence considered at lower k values for comparison.

Overall, the χ(k) representation of the full XAFS spectra in figure 2a of both arsenic containing spectra show similarity. In detail, however, there is a slight difference in wave pattern particularly at higher k values between 8 A^{-1} and 12 A^{-1}.

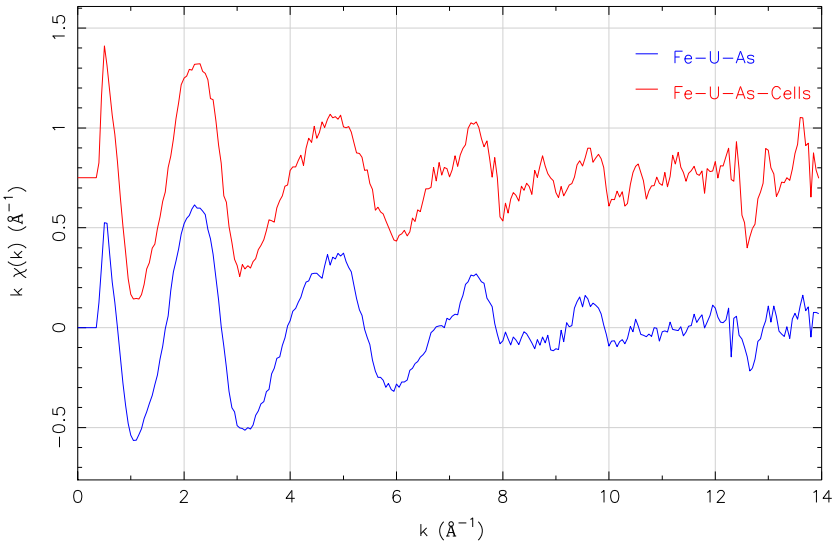

Figure 2a: Comparing arsenic χ(k) experimental samples Fe-U-As to Fe-U-As-bacteria cells up to 9 A^{-1}.

As shown in figure 2b and described in Mbudi et al (2007), it can be inferred that arsenic coordination chemistry is similar to the bonds of As(V) in $As(V)_2O_5$. In fact, the χ(k) comparison clearly reveals the close similarity between the arsenic containing sorption spectra Fe-U-As to Fe-U-As-bacteria cells and the $As(V)_2O_5$ spectrum [19].

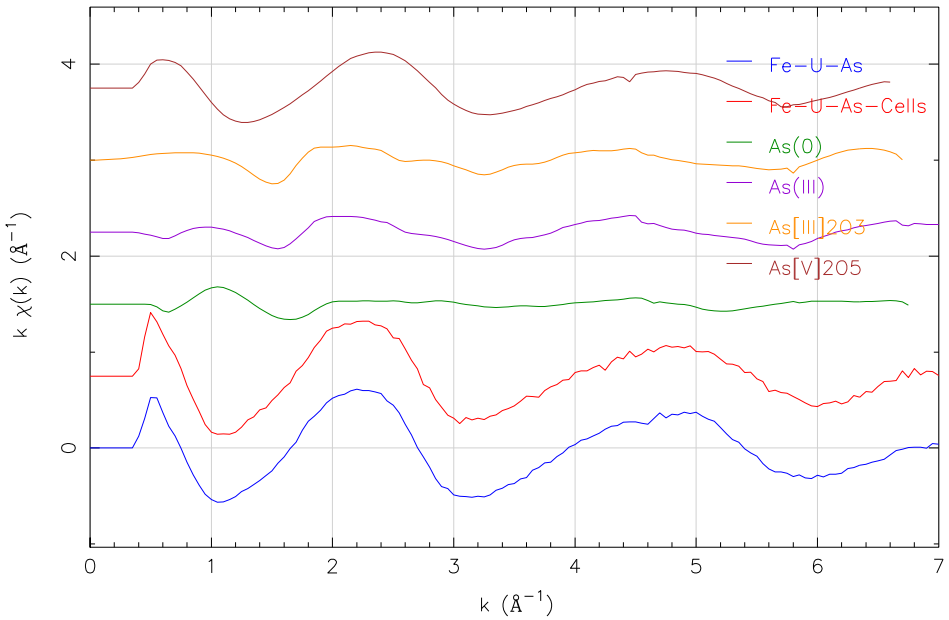

Figure 2b: A comparison of lower portion of less than 7 A^{-1} of k values of the χ(k) arsenic containing experimental samples to references samples of metallic arsenic, arsenic oxide compounds As(III) and As(V).

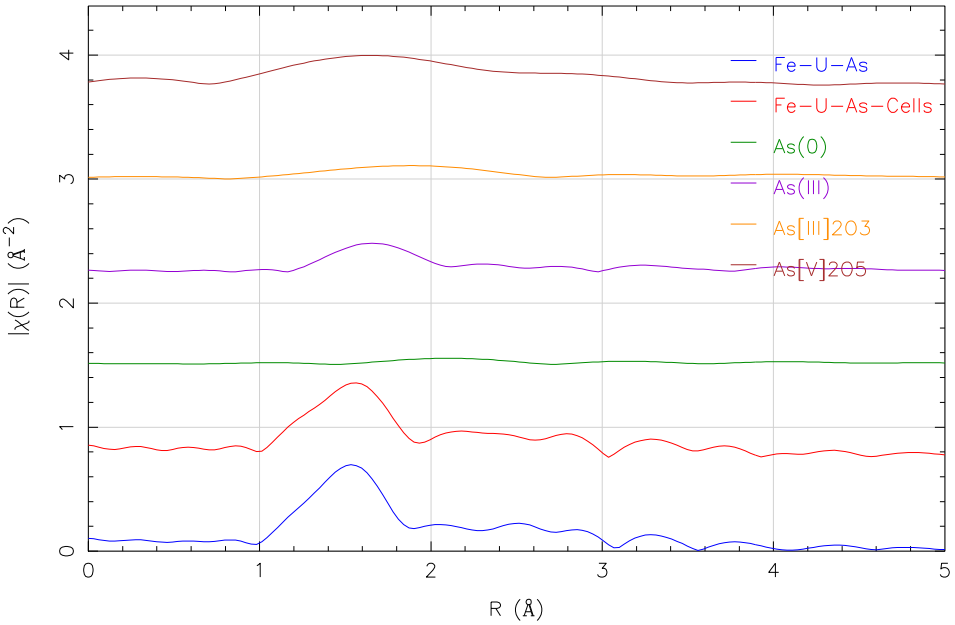

Figure 2c: Fourier transformed χ(k)-spectra of arsenic experimental samples compared to reference compounds.

The FT and backward FT comparisons shown in figure 2c and 2d show similarities between the sorption experiment spectra Fe-U-As and Fe-U-As-bacteria and the arsenate $As(V)_2O_5$ spectrum.

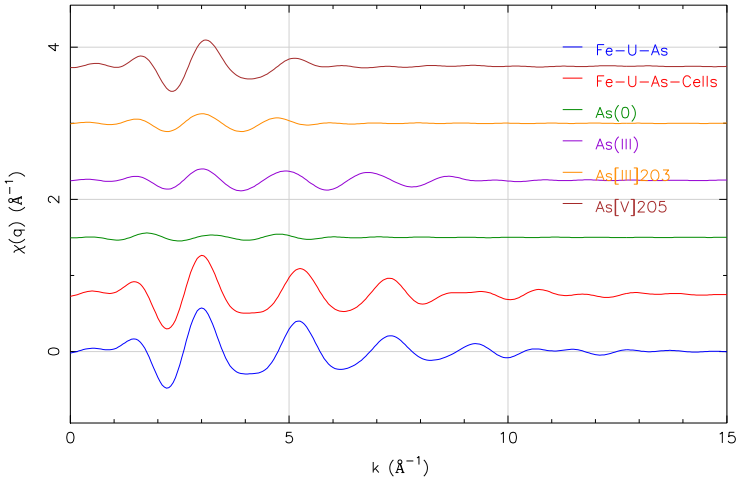

Figure 2d: Backward Fourier transforms of arsenic containing sorption experimental samples spectra compared to reference compounds.

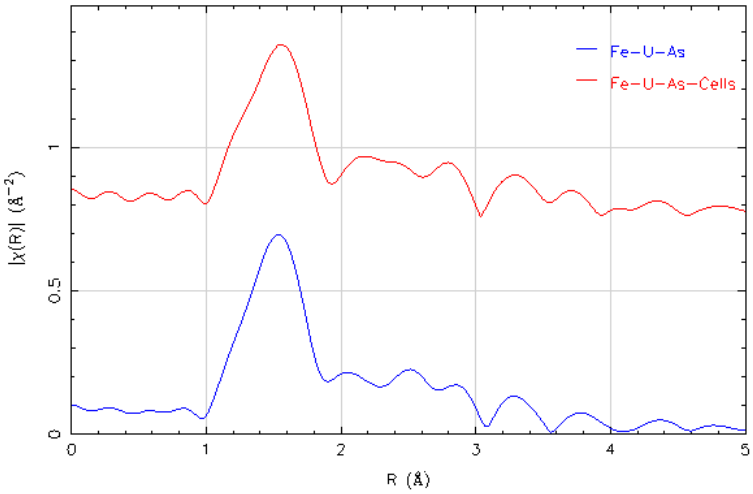

Figure 2e: Fourier transformed arsenic spectra**.**

The magnified FT comparing only the sorption experimental spectra Fe-U-As and Fe-U-As-bacteria shown in figure 2e as well as in figure 2f clearly reveals three main peaks at around respectively 1.6 Å, 2.5 Å and between 2.8 Å and 3 Å. Besides, the k-weighted 1, 2 and 3 comparisons shown in figure 2f do in general not hint to the presence of high atomic number atoms. There is however, a slight trend of amplitudes growth with higher k values.

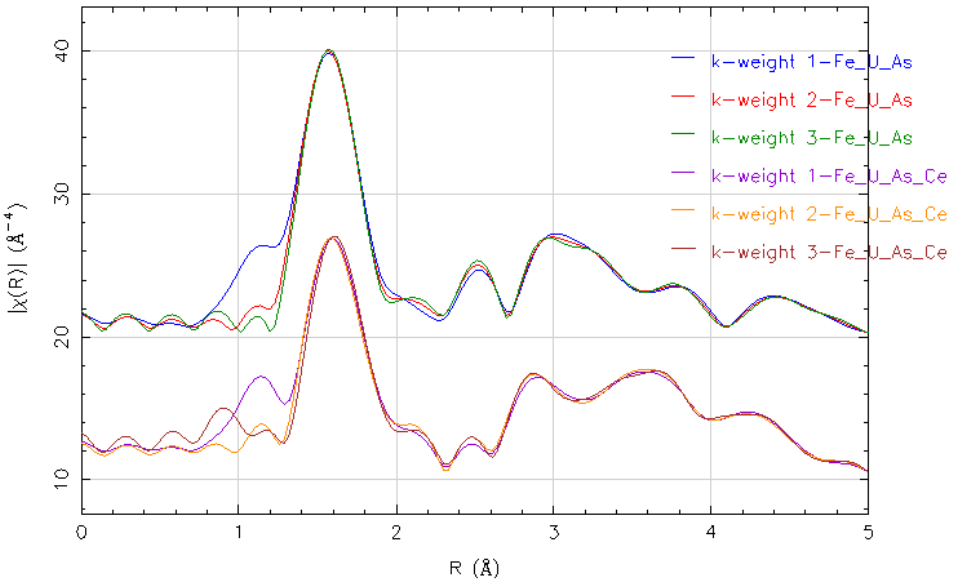

Figure 2f: Comparing k-weights of Fourier transformed arsenic spectra from the systems Fe-U-As and Fe-U-As-bacteria cells.

On the whole, the sorbed arsenic is in pentavalent form coordinated with oxygen atoms in the first two shells. The possible uranium signal beyond the first coordination shell while possible, still however, its occurrence could not be inferred with high precision from k-weighted spectral comparisons

3.2 Quantitative Spectral Analysis

The modeling results of uranium and arsenic EXAFS spectra presented in table 1 are least square fitting respectively based on the theoretical models Schoepite for uranium in the Fe-U system whereas Heinrichite based model with uranium as absorber was used for the systems Fe-U-As and Fe-U-As-bacteria cells. For arsenic spectra, however, Heinrichite was only used for the abiotic system Fe-U-As while Abernathyite was used for the biotic system Fe-U-As-bacteria cells.

Figure 3 illustrates in k space the real part of the Fourier transforms fits of the multi-shell least square fits of experimental EXAFS uranium and arsenic spectra with the respective theoretical models aforementioned. Overall, the theoretical models fit fairly well experimental spectra of both uranium and arsenic particularly at low k values. Figure 4 further illustrates a quite good fit in a classical magnitude-based Fourier transform representation in R space of the multi-shell least square fit of the arsenic spectrum of the abiotic system Fe-U-As.

The modeling of the uranium-based spectrum of the system Fe-U carried out on a k range of 3-10 A^{-1} yields a fairly good fit between experimental data and the Schoepite derived theory particularly for both the first and second coordination shells. Worth mentioning, however, that further attempts to reduce the R factor closer to 0.002 has failed as did related attempts to improve the fit by extending the fitting R space range beyond 2.7 Å with or without the inclusion of multi-scattering paths. This result confirms the bonding of the sorbed uranium to two axial oxygen atoms at a distance corrected of phase shift of 1.7-1.8 Å. The fit of the second coordination shell suggests that the sorbed uranium is most likely coordinated to five equatorial oxygens at a distance 2.2-2.45 Å.

The least square fit of the uranium EXAFS spectrum of the abiotic system Fe-U-As carried out in the k-range 2-9.5 A^{-1} suggests a sorbed structure close to Heinrichite configurations of atoms at least up to more or less 4Å .

Table 1: structural parameters of the respective coordination chemistry of uranium and arsenic sorbed onto metallic iron and Shewanella putrefaciens surfaces compared to the models (MS stands for multiple scattering).

Sample	k-range (A^{-1})	Model	Scatter	N(atoms)	R(Å)	$\sigma^2(Å)^2$	R-factor
Fe-U(U)	3-10	Schoepite	O	2	1.83-1.85	0.0086	0.049
			O-H/O	5	2.29-2.48	0.003	
Fe-U-As(U)	2-9.5	Heinrichite	O	2	1.78-1.8	0.006	0.03
			O	4	2.28-2.95	0.006	
			O(MS)	1	3.4	0.006	
			O(MS)	6	3.61-3.65	0.083	
			As(V)	4	3.76-3.78	0.006	
Fe-U-AS-bacteria cells(U)	2-9.6	Heinrichite	O	2	1.83-1.85	0.003	0.06
			O	4	2.32-2.34	0.003	
			As(V)	4	3.71-3.74	0.06	
Fe-U-As(As)	3-10	Heinrichite	O	4	1.7	0.007	0.05
			O(MS)	12	3-3.1	0.003	
			O	4	3.7		
			U(6)	4	3.7		
Fe-U-AS-bacteria cells(As)	2-12.029	Abernathyite	O	4	1.69	0.002	0.02
			O (MS)	12	3-3.1		
			O	4	3.5		
			U(6)	4	3.6		

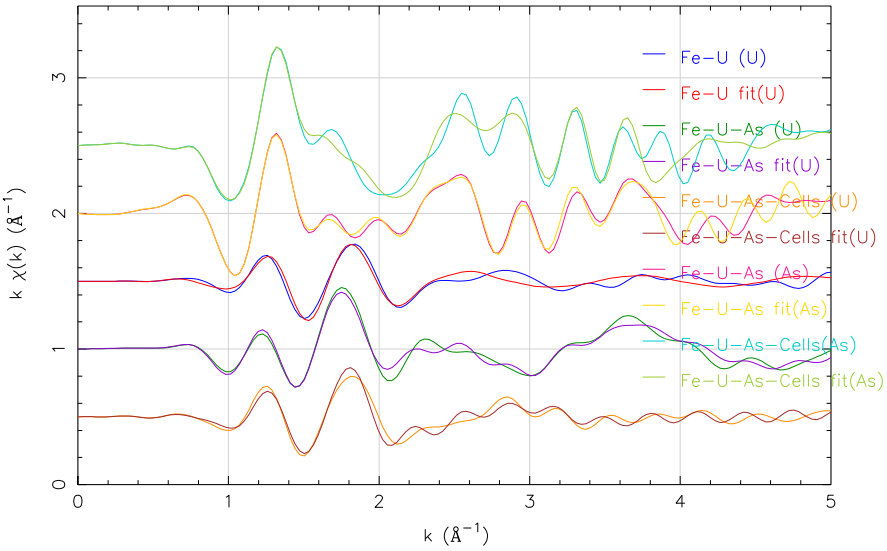

Figure 3: Least Square multi-shell fits of k = 1 weighted experimental spectrum shown in k space after FT of the real components. Peak positions are not corrected for phase shift.

These results also suggest that the sorbed uranium compound in the Fe-U-As system is seemingly associated with two oxygen atoms in linear coordination at a distance of 1.78-1.8 Å and 4 most likely equatorial oxygen atoms at a distance range of 2.28-2.95 Å. This single scattering oxygen-based model was further expanded to include multiple scattering oxygen atoms between 3.4 and 3.65 Å. Further around 3.76-3.78 Å are located similar to Heinrichite, four single scattering arsenic atoms.

The modeling of the EXAFS uranium spectrum for the system Fe-U-As-bacteria cell results in quite similar structural configuration to the aforementioned abiotic system Fe-U-As. However, in the case of Fe-U-As-bacteria cells, the addition of multiple scattering oxygen paths to the model did not improve the overall quality of the fit as attested with a related much higher R factor.

Heinrichite as a model seems to work well with the abiotic system Fe-U-As for both the uranium and arsenic EXAFS spectra. Figure 4 for instance illustrates a quite good fit in a classical magnitude-based Fourier transform of the arsenic EXAFS spectrum of the abiotic Fe-U-As system.

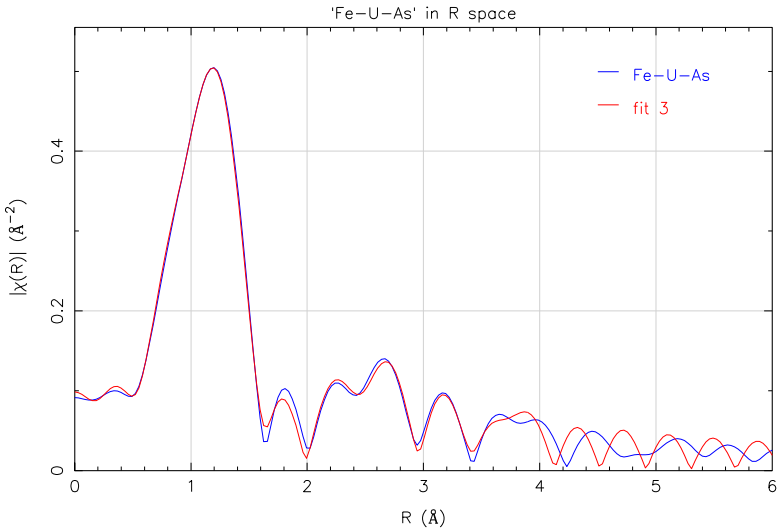

Figure 4: Magnitude of FT based representation of the least square multi-shell fit in R-space of the abiotic arsenic spectrum of the system Fe-U-As system with peak position not corrected of phase shift of about 0.5 Å.

The least square fit of the arsenic spectra for the systems Fe-U-As and Fe-U-As-bacteria cells with respectively Heinrichite and Abernathyite based models suggests in both cases that the absorbing As(V) is surrounded by four oxygen atoms at a distance of 1.69-1.7 Å. Worth mentioning, however, the modeling effort beyond the first

coordination shell for the arsenic spectra appeared to be the most challenging partly because of the unknown configuration between around 1.7 and 3 Å. The inclusion of multiple scattering oxygen paths seems to enhance the overall quality of the fit in the Fe-U-As system but only partly for the Fe-U-As-bacteria cells system. For the latter system, numerous attempts to model it with Heinrichite based system has failed. The use of Abernathyite based model suggests like Heinricite based model that U(VI) scatterers might be responsible for the signals around 3.6-3.7 Å.

4. DISCUSSION

All uranium spectra of the experimental samples, modeled respectively with Schoepite for the Fe-U system and Heinrichite for the Fe-U-As and Fe-U-As-bacteria cells systems have in common their similar configuration for the first coordination shell of U(VI) made of two axial oxygen atoms (uranyl ion) at a distance range of 1.78-1.85 Å. Further, around 2.28-2.95 Å is the domain of the four to five equatorial oxygen atoms consistent with U(VI) coordination and behavior in oxygenated medium. Manceau et al. (1992) gives the respective linear U-O and equatorial U-O shells with peaks at 1.6-1.85 Å and 2.2-2.45 Å. In addition, signals of As(V) scatters for both the Fe-U-As and Fe-U-As-bacteria cells systems may be suggested around 3.7-3.8 Å [1] .

The arsenic spectra for the systems Fe-U-As and Fe-U-As-bacteria cells modeled respectively with Heinrichite and Abernatyhite show a first coordination shell of four single scattering oxygen atoms at 1.69-1.7 Å surrounding As(V) in a tetrahedral configuration. This is consistent with As(V)-(O,OH) well known tetrahedron structural configuration described by Waychumas et al., (1993) and O'Reilly et al., (2001) studying As(V) sorption on HFO. In these arsenic spectra of the systems Fe-U-As and Fe-U-As-bacteria cells, the U(VI) scatters signals may be suggested further away around 3.6-3.7 Å [20, 21].

As clearly shown in figure 1d above comparing the magnitudes of the FT of all uranium spectra, there seems to be no peaks beyond the linear and equatorial U-O/O-OH bonds signatures in the experimental Fe-U system. In addition, in an experimental medium whereby iron and its corrosion products are sorbents, the presence of peaks beyond uranyl equatorial coordination shell might have indicated ($U(VI)O_2^{2+}$) direct bonds with possibility for instance of sharing edges with $Fe(O,OH)_6$ octaedra as mononuclear bidentate inner sphere complexes of HFO functional groups [1]. In addition, as it can be inferred from figure 1e for instance, the presence of U-Fe bond should have been indicated by k dependency with decreasing of the amplitude of the peaks of the FT spectra. Thus, the absence of peaks beyond the equatorial U-O/O-OH bonds in the Fe-U system suggests that surface complexation or chemisorption is not a major sorption mechanism involved but rather the input uranyl has retained its original structure and bonded onto metallic iron surface as ($U(VI)O_2^{2+}$) complexes as precipitates/co-precipitates. Figure 1d also suggests, however that Schoepite with its minor but visible peaks beyond the U-O/U-OH axial and equatorial peaks is much more complex than the experimental Fe-U system. In fact, least square fitting exercise beyond these two peaks using the Schoepite model failed. These observations imply that precipitation/co-precipitation must be a major sorption mechanism for the system Fe-U system. This precipitation/co-precipitation mechanism as major control of uranium behavior can also be drawn from the Fe-U-As and Fe-U-As-bacteria cells systems from both the uranium and arsenic spectra. In these Fe-U-As and Fe-U-As-bacteria cells systems, unlike the Fe-U system, several peaks are clearly spotted beyond the main respectively U-O/U-OH in uranium spectra and As-O/OH peak in arsenic spectra. This observation suggests that mechanisms such as surface complexation or precipitation/co-precipitation may be responsible for some or all of these peaks. Also, as shown in figure 3 and more clearly in figure 4, the uranyl-arsenate mineral Heinrichite as model matches well the experimental data containing both uranium and arsenic at least up to around 4 Å suggesting the preponderant likelihood of precipitation/co-precipitation as leading mechanism.

Worth mentioning however, that for the arsenic spectrum Fe-U-As-bacteria cells, the fitting with Heinrichite failed. Alternatively, a quite fairly good fit could be achieved using the uranyl arsenate Abernathyite as model but for a much-extended k range of 2-12.029 which might include artifacts as aforementioned. Thus, the reliability of the fit at higher k values may be questionable. Overall, the uneasy modeling of the biotic system Fe-U-As-bacteria cells for both the uranium and arsenic spectra suggests the complexity of this experimental system. The likelihood of a similar but slightly different model is plausible in this particular case.

Furthermore, Mbudi et al., (2007) in the XANES fingerprinting have discussed the no occurrence of uranium or arsenic reduction by Fe(0), Fe(II), H_2 nor by Shewanella putrefaciens surfaces [19]. In a nutshell, for the abiotic system Fe-U and Fe-U-As the no reduction of neither U(VI) nor As(V) has been explained by the relatively short hydration time (six hours) and equilibration time (24 hours) which might not have led to sustainable reducing conditions capable of achieving neither U(VI) nor As(V) reduction. For the biotic system Fe-U-As-bacteria cells however, the no reduction of neither U(VI) nor As(V) by Shewanella putrefaciens surfaces has been attributed to the use of nitrate which might have caused conditions that inhibit reducing capabilities of the bacterium cells. Cooper et al., (2003) has shown that NO_3^- is an inhibitor of Fe(III) reduction by Shewanella putrefaciens [23]. Similarly, Rademacher (2006) also observed that the presence of nitrate inhibited Anaeromyxobacter dehalogenans and Geobacter sulfurreducens cells growth and uranium reduction capabilities [22]. In fact, in the Fe-U-As-bacteria cells systems, the toxicity of the relatively high

concentration of the As(V) input fused with nitrate induced inhibition may have led to the limited production of cytochromes for higher Fe(III) reductase activity as inferred from Myers and Myers (1992) [24].

The plausibility of the precipitation/co-precipitation mechanism as leading control of uranium behavior alone or in the presence of arsenic onto metallic iron and Shewanella putrefaciens surfaces is also consistent with geochemical speciation calculations. In bi-component uranium and arsenic systems for instance, the prevalence of uranyl-arsenates species $UO_2H_2AsO_4^+$ and $UO_2(H_2AsO_4)_2$ made the Fe-U-As system prone to the predicted precipitation/co-precipitation of uranium at concentrations as low as 4.45 µM of both initial input of U(VI) and As(V). However, uranyl-carbonate complexes may have played an important role in the biotic system Fe-U-As-bacteria cells which may also explain the uneasy modeling of the related uranium and arsenic spectra using either uranyl arsenates Heinrichite or Abernathyite as model compounds.

5. CONCLUSION

On the whole, EXAFS spectra modeling and analysis has confirmed the presence and prevalence of respectively U(VI)-O/O-OH axial and equatorial bonds in the mono-component uranium system and both U(VI)-O/O-OH and tetrahedron As(V)-(O,OH) in the bi-components uranium-arsenic systems sorbed onto scrap metallic iron and Shewanella putrefaciens surfaces. The absence of peaks beyond the major axial and equatorial U(VI)-O/O-OH bonds in the mono-component uranium system and the concurrent occurrence of U(VI)-O/O-OH and As(V)-(O,OH) bonds in the bi-component uranium-arsenic systems suggest the likely plausibility of precipitation/co-preciptation mechanism as the leading control of uranium behavior.

Acknowledgements: This work was supported by the European Commission – Research Infrastructure Action under the FP6: Structuring the European Research Area (Integrating Activity on Synchrotron and Free Laser Science (IA-SFS) RII3-CT-2004-506008). We thank the Forschungszentrum Karlsruhe's Institut für Synchrotronstrahlung for providing the beamtime and the Institut für Nukleare Entsorgung for providing the necessary technical support from the inception of this project. The author extends his gratitude to the European Network of Excellence for Actinide Sciences, the European Commission Cost Action 629 and the TU Bergakademie PHD Program in Environment, Material science, Technology and Management for their financial assistance to cover the travel and living expenses related to this project and subsequent training.

6. REFERENCES

1. Manceau A., Charlet L., Boisset M.C., Didier B., Spadin L. Sorption and speciation of heavy metals on hydrous Fe and Mn oxides. From microscopic to macroscopic. Applied Clay Science,1992,7: 201-223
2.Mendes KF, Olivatto GP, de Sousa RN, Junqueira LV, Natural biochar effects on sorption desorption and mobility of diclosulam and pendimethalien in soil, Geoderma, 2019, 347, 118-125
3. Ram, Journal of Hazardous Materials, Understanding the mobility and retention of uranium and its daughter products https://doi.org/10.1016/j.jhazmat.2020.124553
4.Lovley, D.R., Philipps E.J.P. Bioremediation of uranium contamination with enzymatic uranium reduction. Environmental Science and Technology,1992,26: 2228-2234
5.Lovley D.R. Bioremediation of organic and metal contaminants with dissimilatory Metal reduction. Journal of Industrial Microbiology,1995,14: 85-93
6.Bostick, D., Jarabek, I., Slover, A., Fiedor, N., Farrel, J., Helferich R. Zero-Valent Iron and metal oxides for removal of soluble regulated metals in contaminated groundwater at a DOE site; U.S. Department of Energy K/TSO-35p; Oak Ridge, TN,1996, pp 1-64
7.Fiedor J.N., Bostick W.D., Jarabek R. J., Farrell J. Understanding the mechanism of Uranium removal from groundwater by Zero-Valent Iron using X-ray Photoelectron Spectroscopy. Environmental Science andTechnology,1998,32(10):1466-1473
8.Gu B., Liang L., Dickey M.J., Yin X., Dai S. Reductive Precipitation of Uranium (VI) by Zero-Valent Iron. Environm. Sci. Technolology,1998, 32 :3366-3373
9.Abdelouas A., Lutze W., Nutall H.E., Gong W. Réduction de l'uranium (VI) par le fer métallique : application à la dépollution des eaux. Comptes Rendus de l'Académie des Sciences de Paris/Earth Planet. Sci., 1999,328:315-319
10.Noubactep C., Meinrath G., Dietrich P., Merkel B. Mitigating uranium in groundwater: prospects and limitations. Environmental Science and Technology,2003,37: 4304-4308
11.Noubactep C., Schöner A., Meinrath G. (2006) Mechanism of uranium removal from the aqueous solution by elemental iron. Journal of Hazardous Materials,2006, B132: 202-212
12.McRae C.W.T., Blowes D.W., Ptacek C.J. In situ removal of arsenic from groundwater using permeable reactive barrier: A laboratory study. Sudbury "99-Mining and the Environment II Conference, September 13-17,1999, Sudbury, Ontario, pp 601-609
13.Su C., Puls R. Arsenate and arsenite removal by Zero valent Iron: Kinetics, redox and transformation, and implication for in situ groundwater remediation. Environmental Science and Technology,2001,35: 1487-1492
14.Mallants D., Diels L., Bastiaens L., Vos J., Moors H., Wang L., Maes N., Vandenhove H. Removal of uranium and arsenic from groundwater using six different reactive materials: assessment of Removal Efficiency. In Merkel B., Planer-Friedrich B., & Wolkersdorfer C. (Eds.) Uranium in the Aquatic Environment. Proc. of the Intern. Conference Uranium Mining and Hydrogeology III and the Intern. Mine Water Association Symposium Freiberg, Germany, September15-21,2002, Springer, Berlin
15.Brown G.E. Jr. Spectroscopic studies of chemisorption reaction mechanism at oxide-water interfaces. In Hochella M.F. Jr. and White A.F. (Editors), Mineral-Water Interface Geochemistry, Reviews in Mineralogy, Mineralogical Society of America, 1990, 23: 309-364
16.Denecke M.A., Janssens K., Proost K., Rothe J., Noseck U. Confocal Micrometer-Scale X-ray Fluorescence and X-ray Absorption Fine Structure Studies of Uranium Speciation in a Tertiary Sediment from a Waste Disposal Natural Analogue Site. Environmental Science and Technology,2005,39(7): 2049-2058
17. Ravel B., Newville M. Athena, Artemis, Hephaestus: Data Analysis for X-ray Absorption Spectroscopy using IFEFFIT. Journal of Synchrotron Radiation.2005,12, 537-541
18. Rothe J., Denecke M.A., Dardenne K., Fanghänel Th. The INE-beamline for actinide research at ANKA. Radiochimica Acta,2006,94: 691-696
19.Mbudi C., Brendenbach B., Merkel B., Behra P. Speciation of Uranium and Arsenic Sorbed onto Scrap Metallic Iron and Shewanella putrefaciens Surfaces: A XANES Fingerprinting Investigation. Wissenschaftliche Mitteilungen, Inst. Geol. TU BAF,2007,35:35-42, Freiberg
20.Waychumas G.A., Rea B.A., Fuller C.C., Davis J.A. Surface chemistry of ferrihydrite: Part 1. EXAFS studies of the geometry of coprecipitated and adsorbed arsenate. Geochimica et Cosmochimica Acta,1993, Vol 57: 2251-2269
21.O'Reilly S.E., Strawn D.G., Sparks D.L. Residence time effects on arsenate adsorption/desorption mechanisms on goethite. Soil Science Society of America

Journal,2001,65: 67-77
22.Rademacher L.K., Lundstrom C. C., Johnson T.M., Sanford R. A., Zhao J., Zhang Z. Experimentally determined uranium isotope fractionation during reduction of hexavalent U by bacteria and zero valent iron. Environmental Science and Technology,2006,40: 6943-6948
23.Cooper D., Pcardal F., Schimmelmann A., Coby A. Chemical and Biological interactions during Nitrate and Goethite reduction by Shewanella putrefaciens. Applied and Environmental Microbiology,2003, 69: 3517-3525
24.Myers, C.R., Myers J.M. Localization of Cytochromes to the Outer Membrane of Anaerobically Grown Shewanella putrefaciens MR-1. FEMS Microbiology Letters.1992, 114: 215-222.

Cite this article: N'zau Umba-di-Mbudi, Clement. INVESTIGATING THE MECHANISMS OF U(VI) SORPTION ONTO FE(0) AND SHEWANELLA PUTREFACIENS SURFACES IN THE PRESENCE OF AS(V) USING EXTENDED X-RAY ABSORPTION FINE STRUCTURE SPECTROSCOPY. *Am. J. innov. res. appl. sci. 2021; 12(6): 231*-243.